Supplementary Information

Engineering Novel Cuboctahedral N-doped C Coated p-CuO/n-TiO_2 Heterojunction Toward High-Performance Photocatalytic Cross-Dehydrogenative Coupling

Shuo Zhou, † Qiuyan Shen, † Feng-Lei Yang,* Wenwen Zhan, Xiaojun Wang, Xiguang Han*

Jiangsu Key Laboratory of Green Synthetic Chemistry for Functional Materials, School of Chemistry and Material Science, Jiangsu Normal University, Xuzhou, Jiangsu 221116, P. R. China

E-mail: yangfl@jsnu.edu.cn, xghan@jsnu.edu.cn

†These authors contributed equally

1. Experimental details

1.1 Synthesis of Cu-MOF-199 (HKUST-1) precursors

First, $Cu(NO_3)_2 \cdot 3H_2O$ (0.024 g, 0.1 mmol) was dissolved in the mixed-solvent of 4.5 mL ethanol and 4.5 mL N,N-dimethylformamide (DMF) to obtain solution (a). Then, benzimidazole (0.201g, 1.7 mmol) was added to the same mixed-solvent (4.5 mL ethanol and 4.5 mL DMF) to obtain solution (b). Solution (b) was added to solution (a) to form the bright blue solution (c), which was agitated for 10 min. 1,3,5-Benzenetricarboxylic acid (0.021 g, 0.1 mmol) was added to the mixed-solvent of 9 mL ethanol and 9 mL DMF to obtain solution (d). Solution (d) was added to solution (c) and agitated for 6 h at 90 °C. Finally, HKUST-1 was obtained by centrifuging, washing three times with anhydrous ethanol, and drying at 60 °C in an oven.

1.2 Preparation of CuO@N-C

The CuO@N-C sample was synthesized via calcination of the obtained HKUST-1 at 500 °C for1 h with heating rate of 5 °C·min^{-1} in the Ar atmosphere.

1.3 Preparation of CuO-TiO_2@N-C

In a typical synthesis, HKUST-1 (0.01g) and isopropyl titanate (0.134 mmol) were dissolved in the mixed-solvent of 5 mL ethanol and 5 mL N,N-dimethylformamide (DMF). After stirring by ultrasonic concussion for 10 minutes, the mixture was transferred to a 25 mL reaction kettle and placed in an oven at 150 ^{o}C for 6 hours. After reaction, the product Ti-HKUST-1 was collected via centrifugation, washed several times with fresh ethanol, then dried at 60 °C overnight. The CuO-TiO_2@N-C sample was synthesized via calcination of the obtained above samples at 500 °C for 1h with heating rate of 5 °C·min^{-1} in the Ar atmosphere.

Adding titanium-tetraisopropanolate (TIP) precursor along with $Cu(NO_3)_2 \cdot 3H_2O$ will affect the nature of the production formation, at least the appearance has changed (Fig. S4).

1.4 Preparation of TiO_2@N-C

In a typical synthesis, 2-Aminoterephthalic acid (0.070 g, 0.39 mmol) was dissolved

in 3 mL of methanol and 7 mL of N, N-dimethylformamide (DMF). After stirring for 10 minutes by ultrasonic shaking, isopropyl titanate (75 ul, 0.28 mmol) was added, and the mixture was transferred to a 25 mL Teflon-lined steel autoclave and placed in an oven at 150 ° C for 24 hours under static conditions. After reaction, the product was collected via centrifugation and washed several times with fresh ethanol, then dried at 60 °C overnight. The TiO_2@N-C sample was synthesized via calcination of the obtained above samples at 550 °C for 1h with heating rate of 2 °C·min^{-1} in the O_2 atmosphere.

The use of the same acids (1,3,5-Benzenetricarboxylic acid) as in the CuO@N-C synthesis, along with isopropyl titanate, does not result in the formation of uniformly shaped Ti (Fig. S8) compounds containing organic ligands. However, by using 2-Aminoterephthalic acid, it is possible to obtain the desired TiO_2@N-C material with a similar nitrogen-doped carbon layer as CuO@N-C, since they exhibit similar ID/IG ratio (1.38 and 1.31) as shown if Fig. S11.

1.5 Characterization

The composition and phase of the as-prepared products were acquired by the powder X-ray diffraction (XRD) pattern using a Panalytical X-pert diffractometer with Cu K_α radiation. The morphology and crystal structure of as-prepared products were observed by scanning electron microscopy (SEM, SU8100), and high-resolution transmission electron microscopy (HRTEM, FEI Tecnai-F20) with an acceleration voltage of 200 kV. All TEM samples were prepared from depositing a drop of diluted suspensions in ethanol on a carbon film coated copper grid. PHI QUANTUM2000 photoelectron spectrometer (XPS) was using to characterize the surface compositions of product. The surface areas of these samples were measured by the Brunauer-Emmett-Teller (BET) method using nitrogen adsorption and desorption isotherms on a Micrometrics ASAP 2020 system. The EPR experiments performed with the Bruker ESP-300E spectrometer with X-band at 9.8 GHz and 100 Hz field modulation allowed for the detection and analysis of the free radicals present at the photocatalytic reaction time of 0, 5, 10, 15min.

1.6 Photocatalytic Activity Measurements.

The photocatalyst (5 mg), tetrahydroisoquinolines (0.05 mmol) and indoles (0.1 mmol) were added into 1 mL CD_3CN. The mixture solution was stirred and irradiated by blue LEDs (λ=450 nm, 3W) for 36 h under atmosphere at room temperature. The yield of the product was characterized by 1H NMR spectra. To perform the recycling experiments, the photocatalyst was recovered by centrifugation and washed with dichloromethane for several times. The recycled photocatalyst was then dried in vacuum at about 60 °C.

1.7 Photoelectrochemical measurements

Photoelectrochemical experiments were measured in the three electrode quartz cell, and catalyst-modified conductive glass (FTO, 25 cm^2) served as a working electrode, $Hg/HgCl_2$ electrode and platinum electrode were used as the reference electrode and counter electrode, respectively. The catalyst ink was prepared by ultrasonically dispersing 5 mg of catalyst into a mixed solution containing 0.5 mL of anhydrous ethanol. Then, 100 μL of the prepared catalyst ink was dropped onto the conductive glass and dried under room temperature. The conductive glass was then dried at 300 °C for 2 h. In the three-electrode cell, added 0.025 M KH_2PO_4 and 0.025 M Na_2HPO_4 standard buffer as the electrolytes. The Linear Sweep Voltammetry（LSV), Amperometric i-t Curve(i-t）and A.C. Impedance（IMP）measurements were carried out on a CHI-760E workstation under 300W Xe arc lamp system was used as the visible-light irradiation source**.**

1.8 Density Functional calculations

All of the density functional calculations were performed using plane-wave pseudopotential method in the framework of DFT+U (U=4 for Cu, U=4.5 for Ti [1]), as implemented in the Quantum Espresso (QE) package Version 7.0 code. [1, 2] The generalized gradient approximation (GGA) with the Perdew–Burke–Ernzerhof (PBE) functional formulation[3] were used to describe the exchange-correlation effects. The ion-electron interaction was described by ultrasoft pseudopotential. A plane-wave kinetic energy cutoff of 500 eV was employed. Partial occupancies of electronic bands were allowed with the Gaussian smearing method with width of 0.01 eV.

The self-consistent convergence accuracy was set at 1.0×10^{-5} eV/atom, and the convergence criterion for the force between atoms was 1.0×10^{-4} eV/Å. The K-Point mesh of 2×1×1 grid, featuring enough accuracy to total energy by convergence test, was used to sample the two-dimensional Brillouin zone for geometrical optimization. The slab models of CuO (-111) surface (CuO--111) and TiO_2 (200) surface (TiO_2-200) were constructed and separated by a >15 Å vacuum in Z direction. 2×7 unit cell of CuO (-111) (a), and 3×2 unit cell of TiO_2 (200) were used to build the CuO-TiO_2 heterostructure layer, mean strain was about 3.5 %.

2. Experimental results

Fig. S1. (a) XRD pattern of the HKUST-1; (b) SEM image of the as-obtained HKUST-1; (c-f) EDX elemental mapping of Cu, O, C, N.

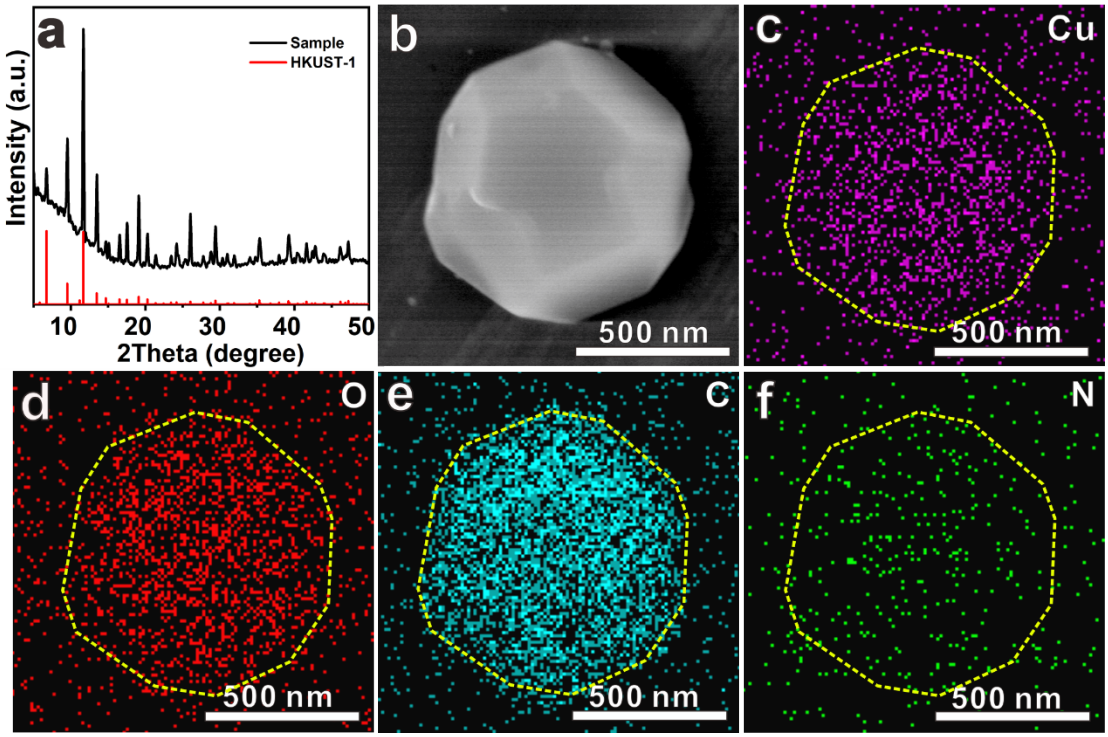

Fig. S2. XRD pattern of cuboctahedral Ti-HKUST-1 precursor (a), FE-SEM images of cuboctahedral HKUST-1 precursor (b) and Ti-HKUST-1 precursor (c).

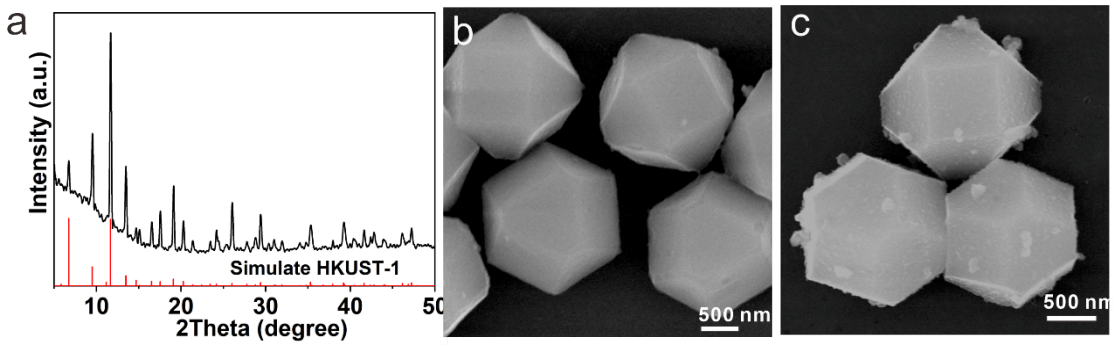

Fig. S3. The EDX mapping of Ti-HKUST-1 precursor.

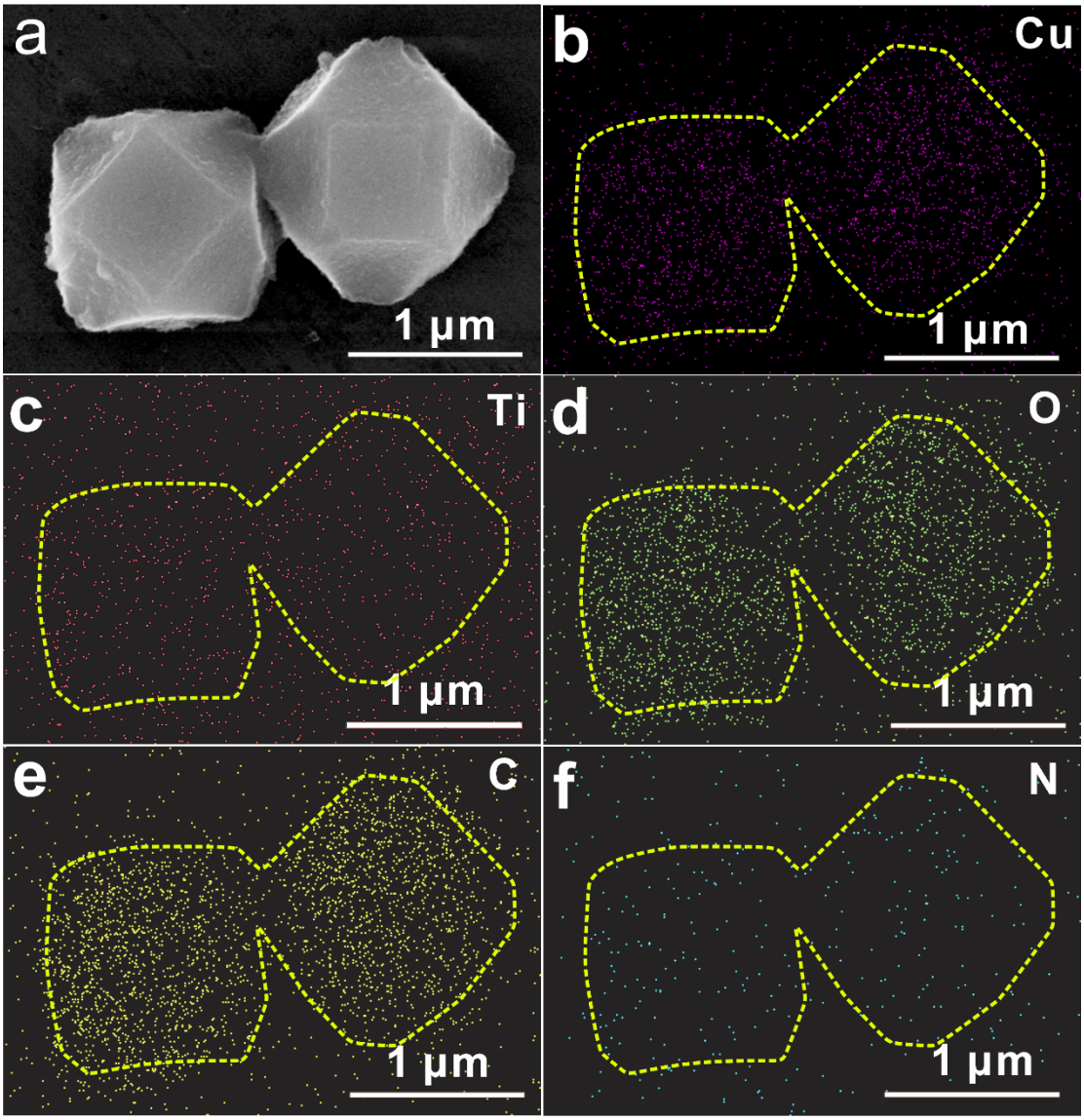

Fig. S4. The SEM image of product obtained by adding TIP precursor along with $Cu(NO_3)_2 \cdot 3H_2O$ during the synthesis of Ti-HKUST-1.

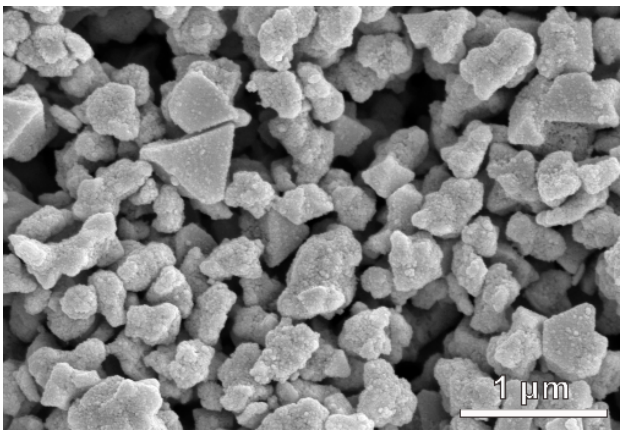

Fig. S5. TGA curves of the as-obtained Ti-HKUST-1 precursor.

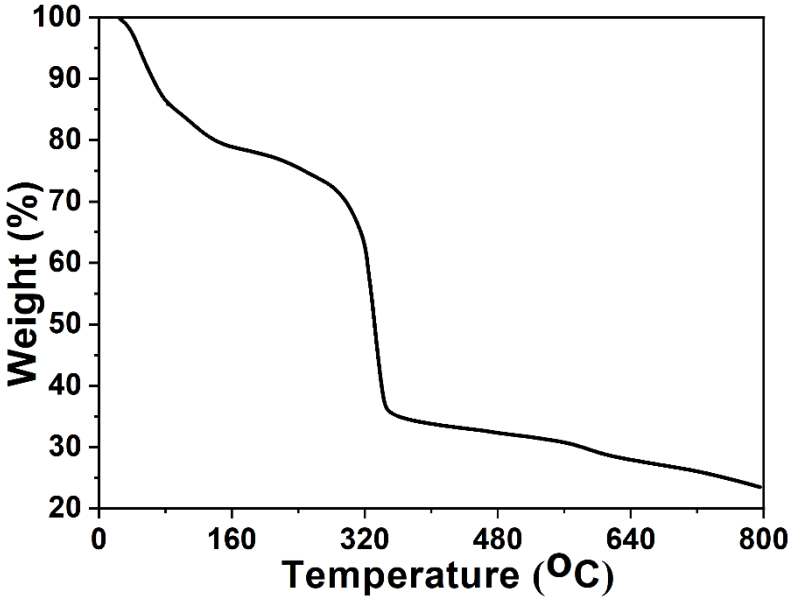

Fig. S6. magnified SEM image of CuO-TiO_2@N-C.

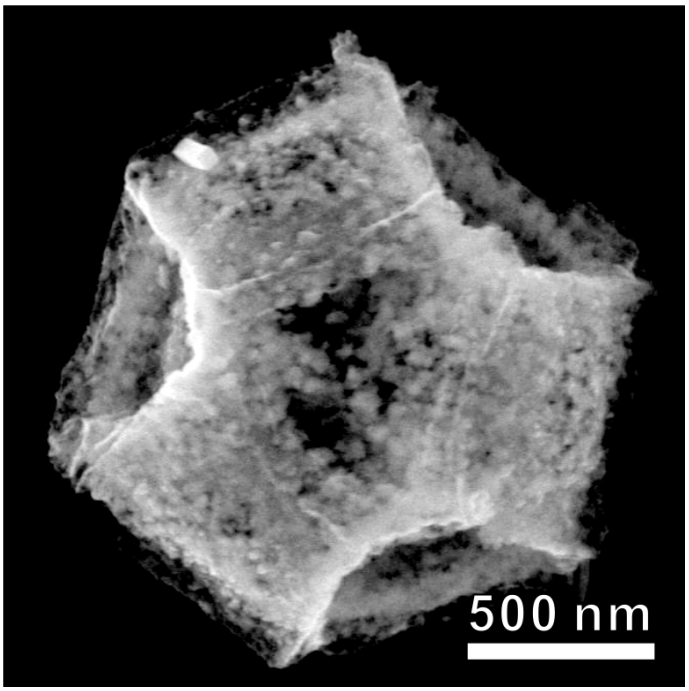

Fig. S7. (a)N_2 adsorption/desorption isotherms and (b) BJH pore size distribution of cuboctahedral CuO-TiO_2@N-C.

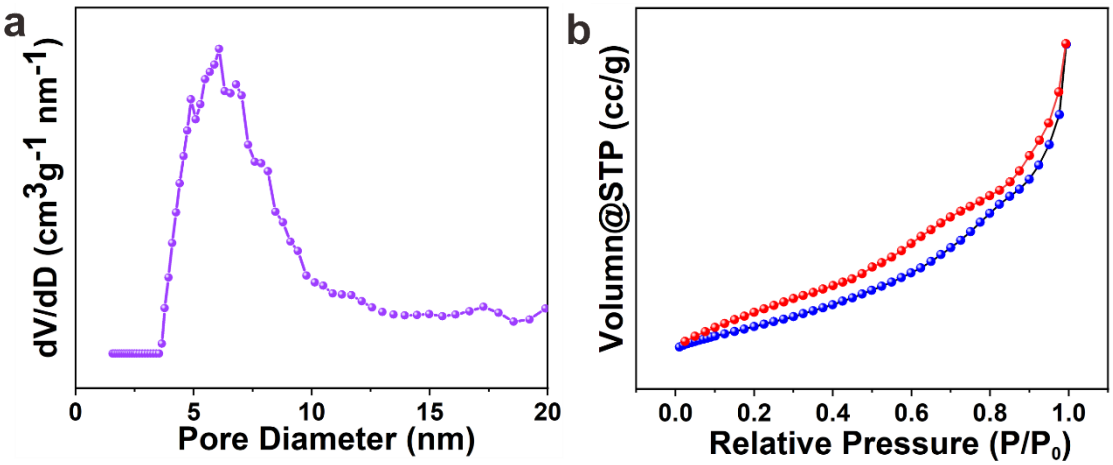

Fig. S8. The SEM image of product obtained by using the same acids (1,3,5-Benzenetricarboxylic acid) as in the CuO@N-C synthesis, along with isopropyl titanate during the synthesis of TiO_2@N-C precursor.

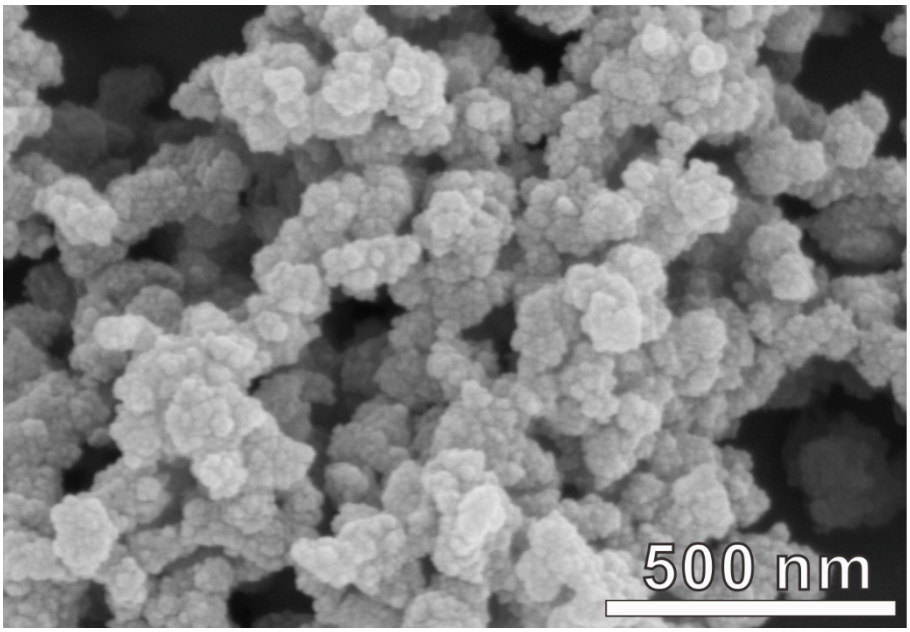

Fig. S9. (a) XRD pattern of the TiO_2@N-C; (b) SEM image of the as-obtained TiO_2@N-C; (c-h) STEM image and EDX elemental mapping of Ti, O, C, N.

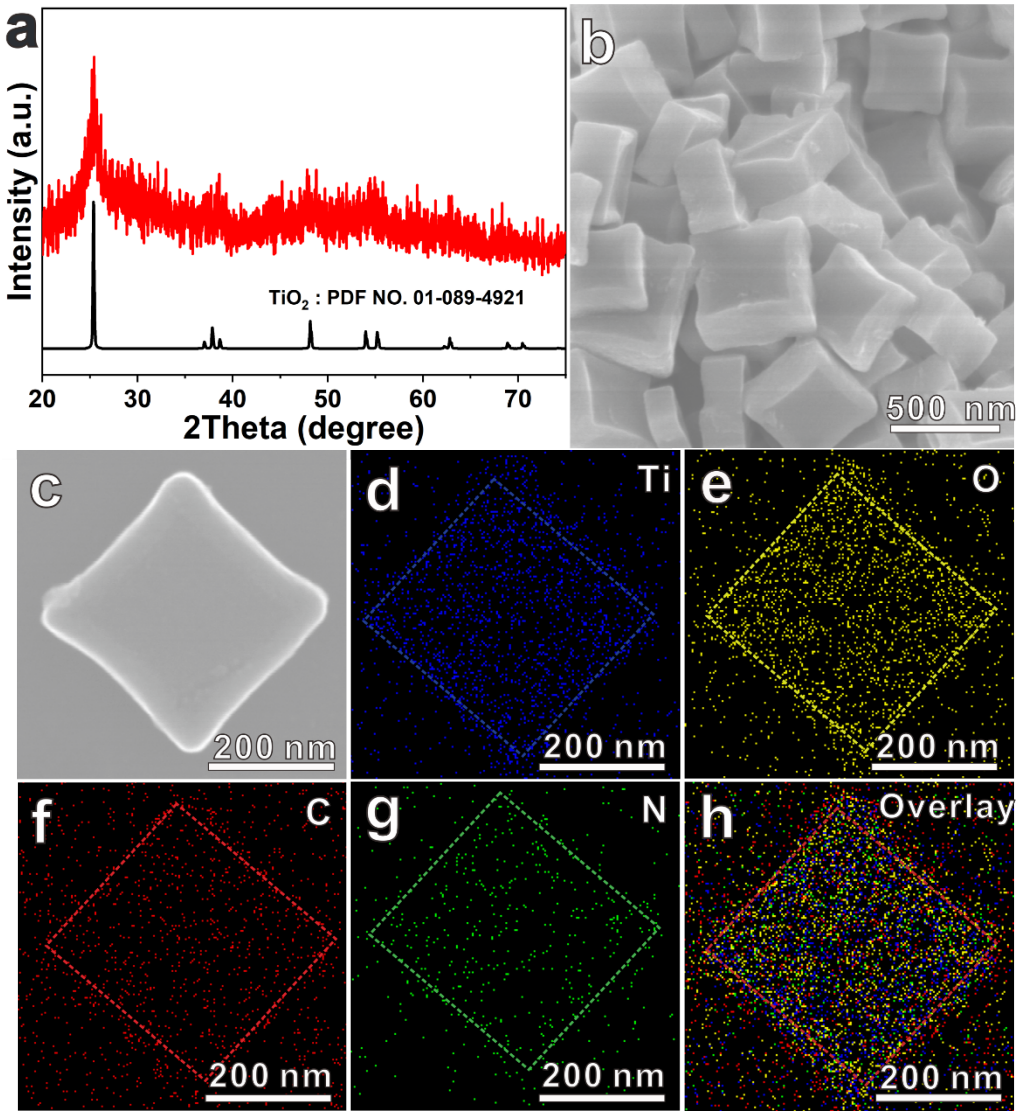

Fig. S10. (a) XRD pattern of the CuO@N-C; (b) SEM image of the as-obtained CuO@N-C; (c-h) STEM image and EDX elemental mapping of Cu, In, O, C, N.

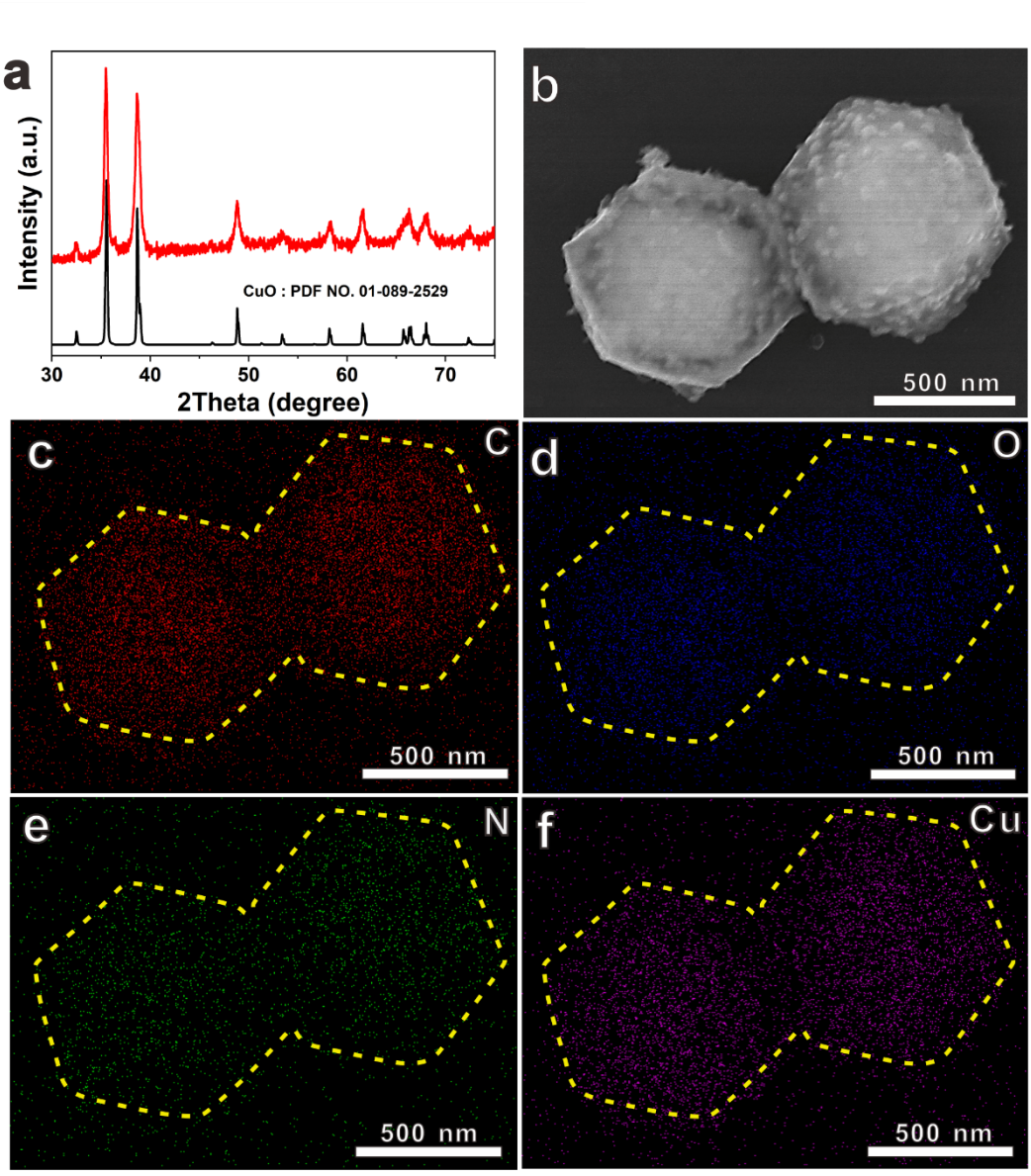

Fig. S11 The ID/IG ratio in Raman spectra for CuO-TiO_2@N-C (a), CuO@N-C (b) and TiO_2@N-C (c)

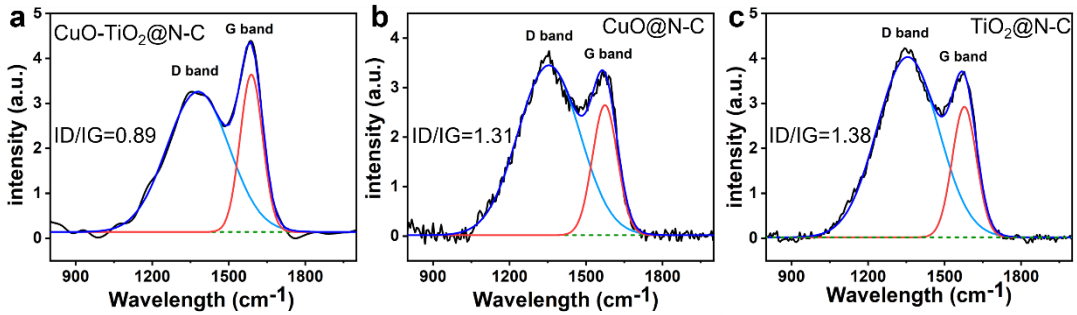

Fig. S12. Survey spectrum of CuO-TiO_2@N-C.

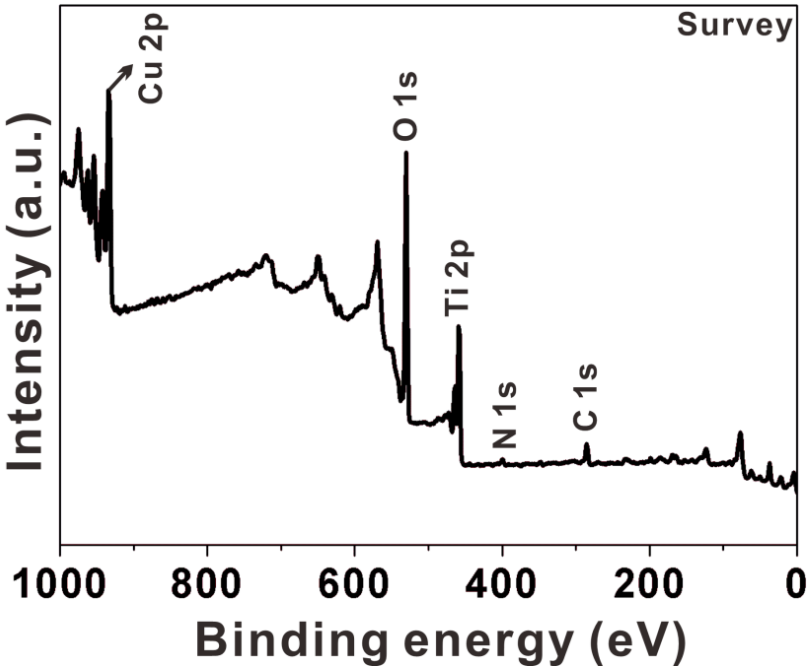

Table. S1 Atomic content of the various elements in CuO-TiO_2@N-C, CuO@N-C and TiO_2@N-C abstracted from XPS-spectra.

Sample	C (Atomic%)	N (Atomic%)	O (Atomic%)	Cu (Atomic%)	Ti (Atomic%)
CuO-TiO_2@C-N	29.45	3.18	52.66	4.72	9.99
TiO_2@C-N	38.92	7.75	40.46	----	12.87
CuO@C-N	67.18	11.74	17.73	3.35	----

Fig. S13 (a) XRD pattern, (b, c) SEM image, (d-h) corresponding elemental mapping of CuO-TiO_2@N-C after catalytic reaction.

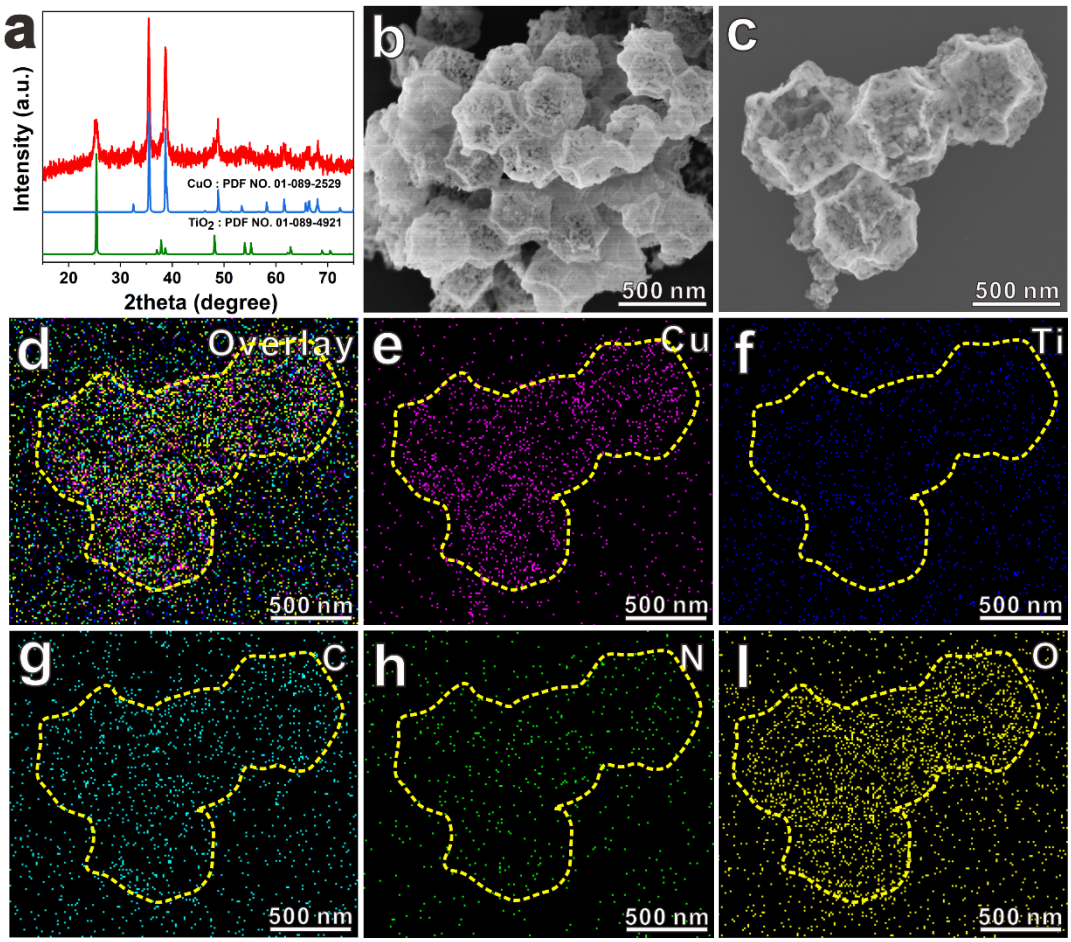

Fig. S14 The oxide states of Cu (a) and Ti (b) analyzed by XPS before and after reactions.

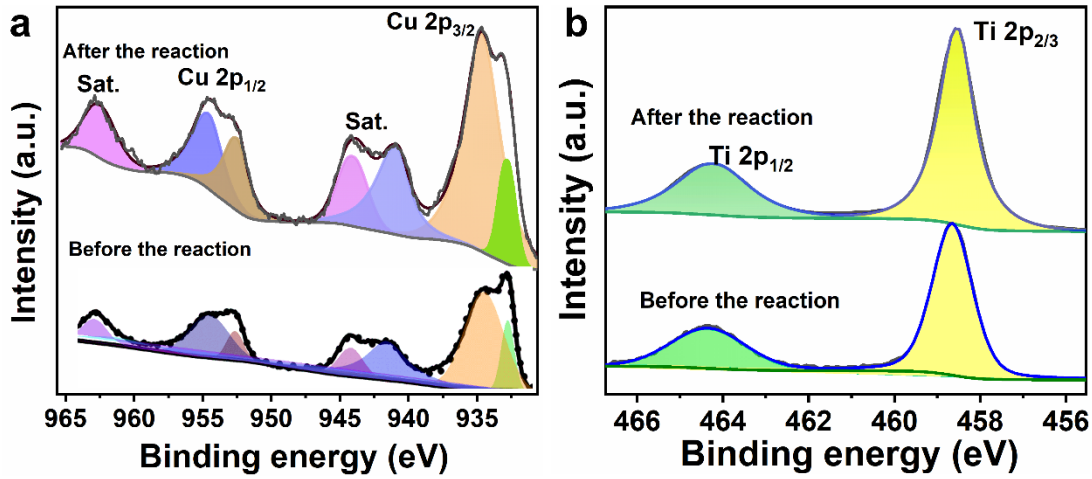

Fig. S15. Product yield in the CDC reaction with different derivatives of indole and N-aryltetrahydroisoquinoline over hollow cuboctahedral CuO-TiO_2@N-C.

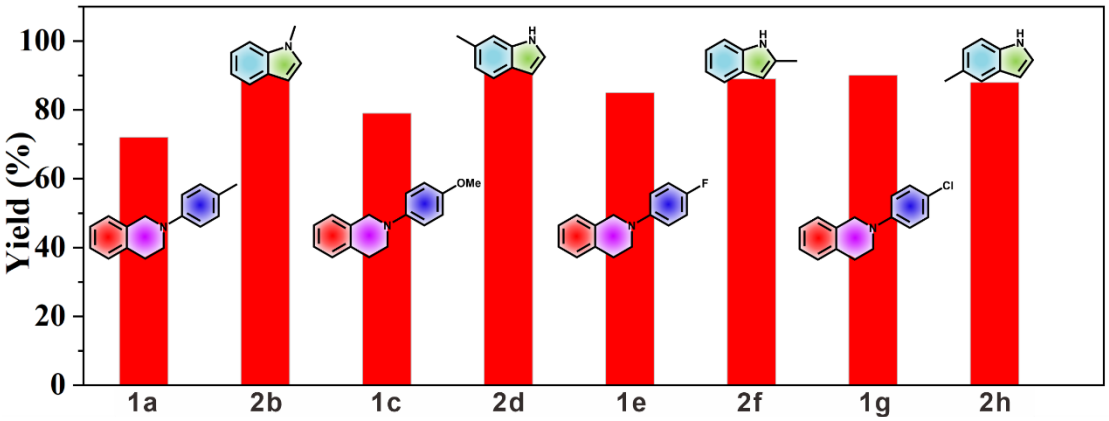

Fig. S16. NMR spectra of the product catalyzed by CuO-TiO_2@N-C annealed at different temperatures (b), by CuO-TiO_2@N-C, CuO@N-C and TiO_2@N-C respectively (b), catalyzed by CuO-TiO_2@N-C with different substituents (c).

(a)

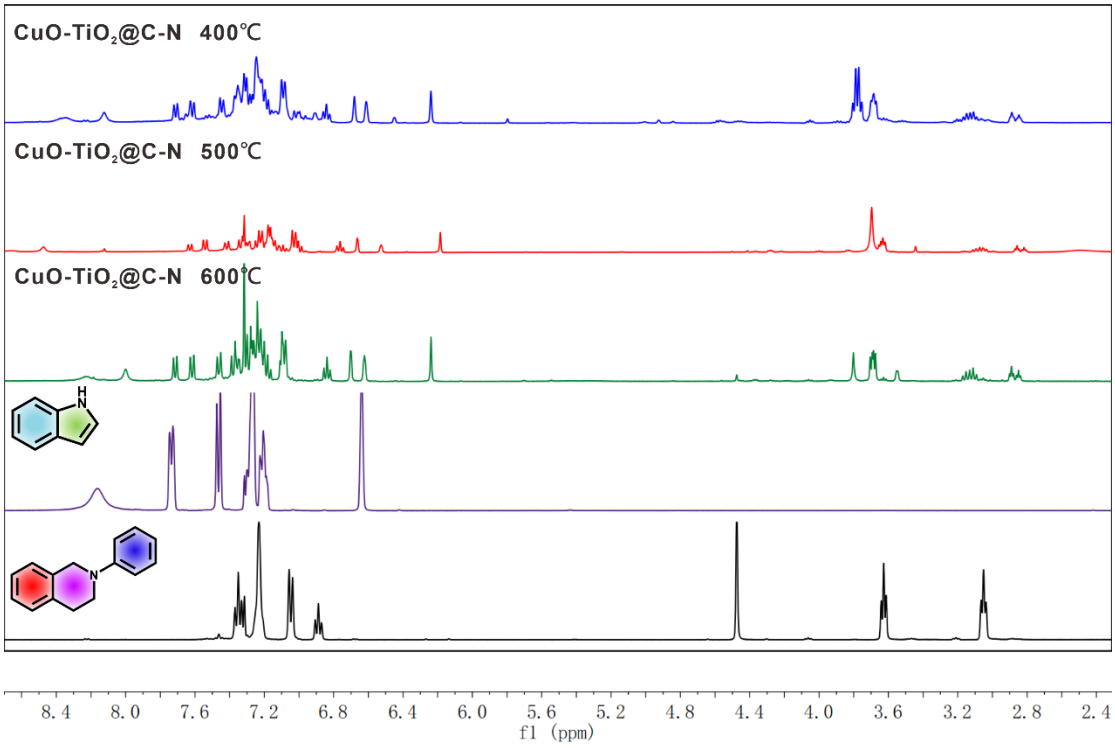

(b)

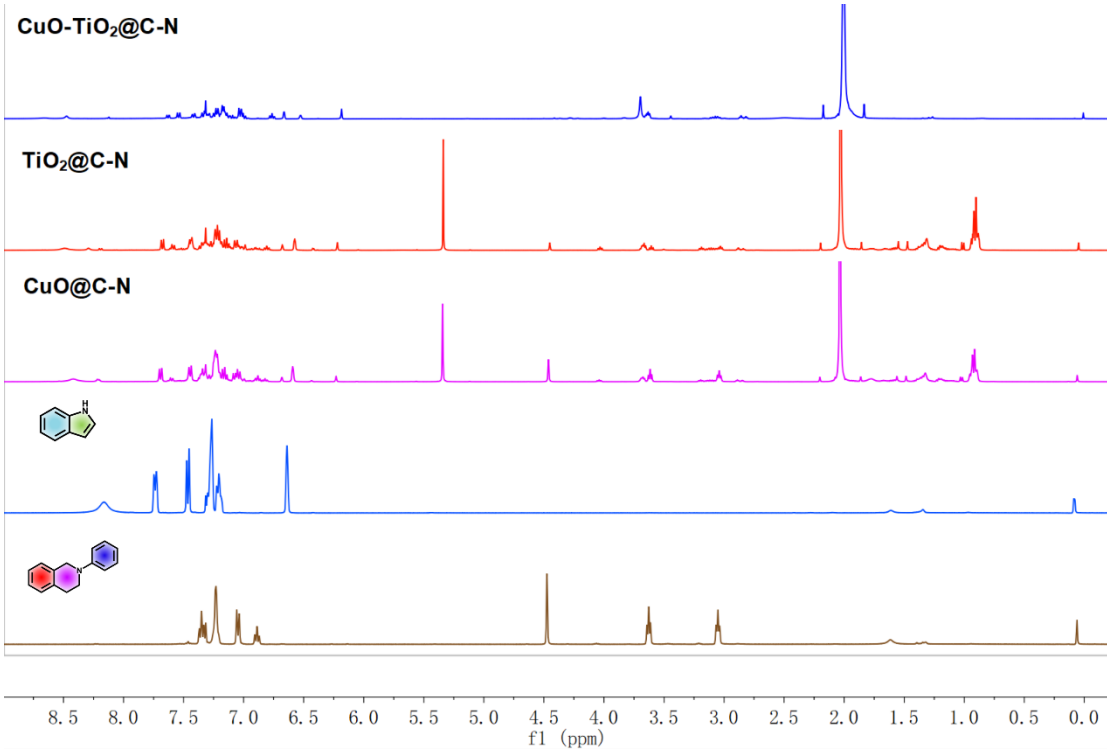
CuO-TiO2@C-N
TiO2@C-N
CuO@C-N
8.5 8.0 7.5 7.0 6.5 6.0 5.5 5.0 4.5 4.0 3.5 3.0 2.5 2.0 1.5 1.0 0.5 0.0
f1 (ppm)

(c)

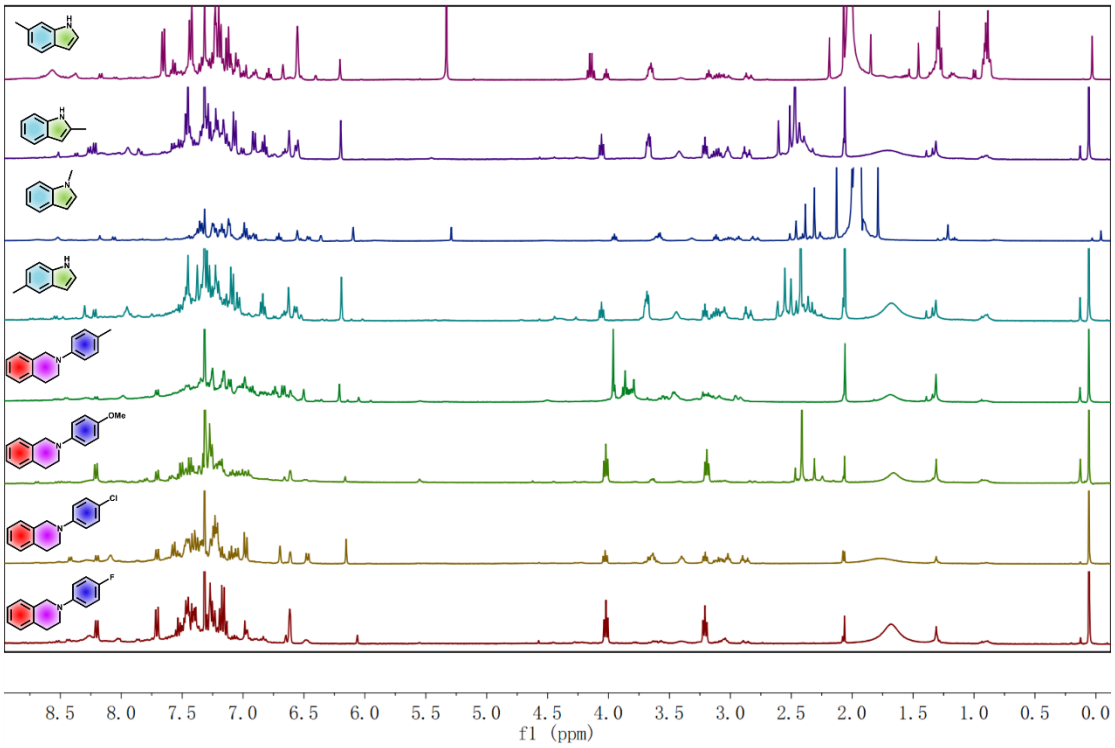
OMe
Cl
F
8.5 8.0 7.5 7.0 6.5 6.0 5.5 5.0 4.5 4.0 3.5 3.0 2.5 2.0 1.5 1.0 0.5 0.0
f1 (ppm)

Fig. S17. Compare the efficiency of CuO-TiO_2@N-C with CuO@N-C and TiO_2@N-C for different derivatives of indole in the CDC reaction.

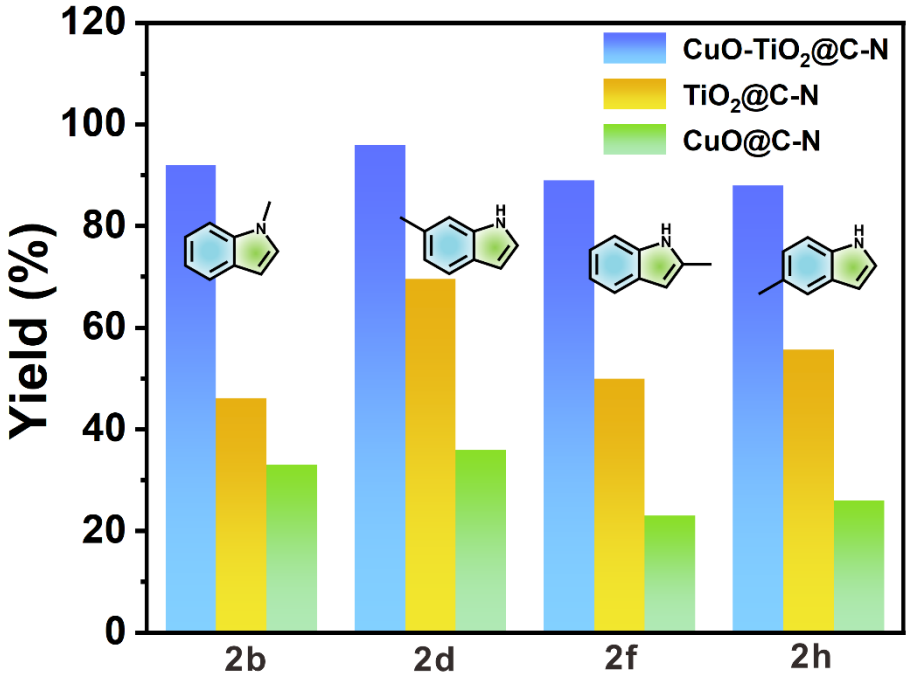

Figure S18 The SEM image of cuboctahedral Ti-HKUST-1 annealed at 400 ^{o}C (a), 500 ^{o}C (b) and 600 ^{o}C (c), respectively.

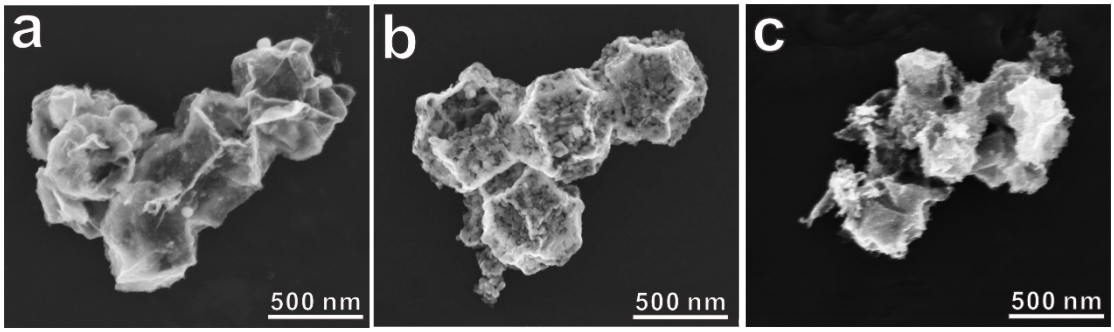

Figure S19 Product yield of the CDC reaction catalyzed by catalysts annealed at different temperatures (cuboctahedral Ti-HKUST-1 annealed at 400 °C, 500 °C and 600 °C, respectively).

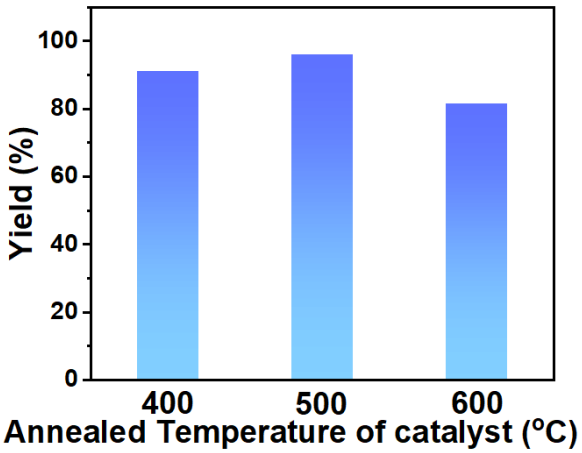

Figure S20 Product yield of the CDC reaction performed in different solvent systems

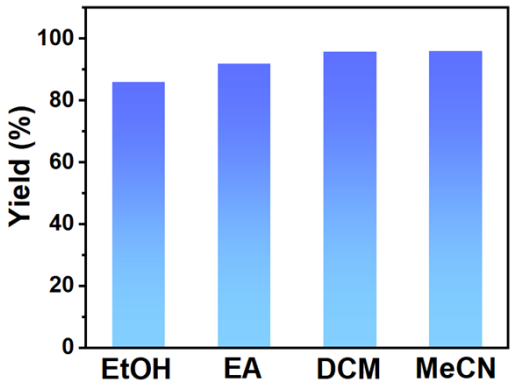

Fig. S21. Comparison of the photocatalytic efficiency of CuO-TiO_2@N-C for CDC reaction under different wavelength of light.

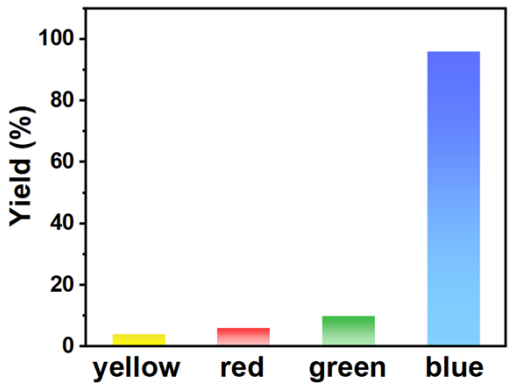

Fig. S22. The DFT model of CuO (-111), and TiO_2 (200) surface supercell were used to build the CuO-TiO_2 heterostructure layer, mean strain was about 3.5 %.

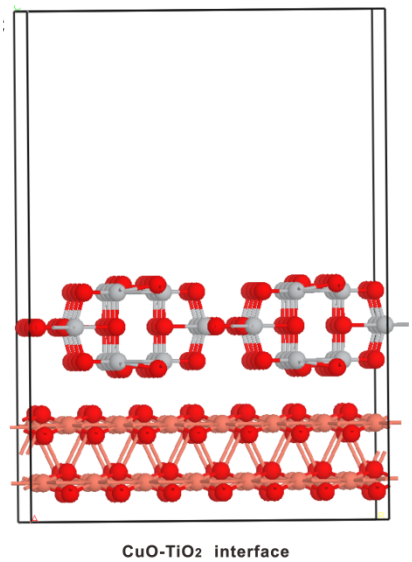

Fig. S23. Electrostatic potentials of individual CuO--111, TiO_2-200 and CuO--111/TiO_2-200 heterostructure.

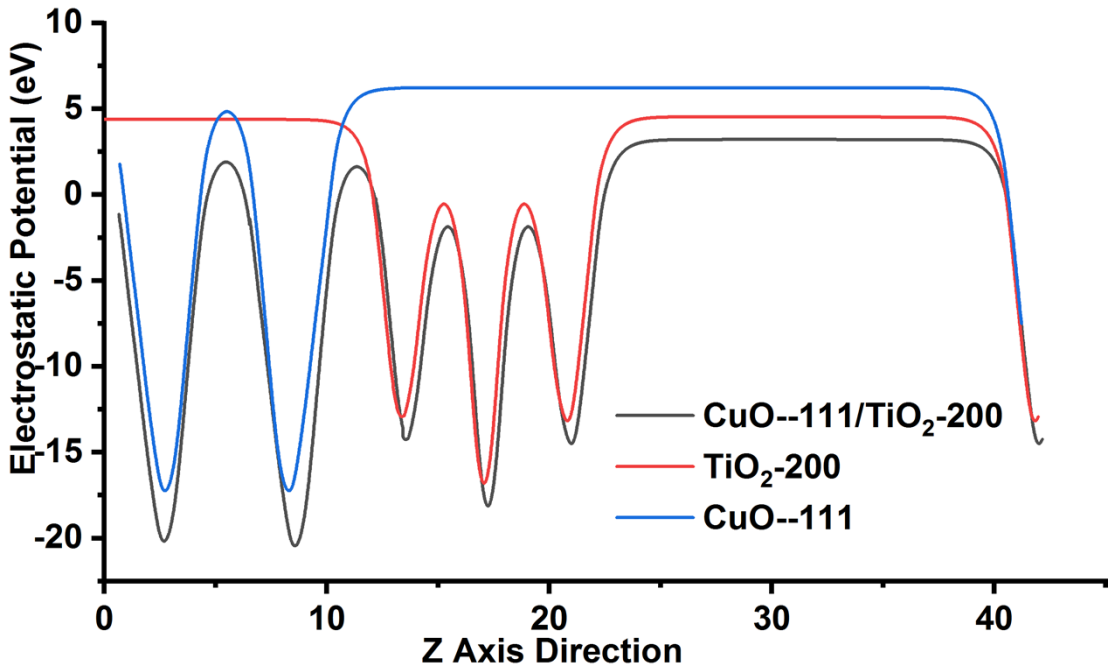

Fig. S24 (a) the charge density difference and of reactant molecules (indole) adsorbed over the composite surface (with cyan-blue and yellow colors representing electron accumulation and depletion, respectively); (b) H-bond formed between adsorbed reactant molecules (indole) and composite surface; (c) PDOS of the graphite (001)/CuO (-111) interface. Inset: C1 the computational model of the graphite (001)/CuO (-111) interface.

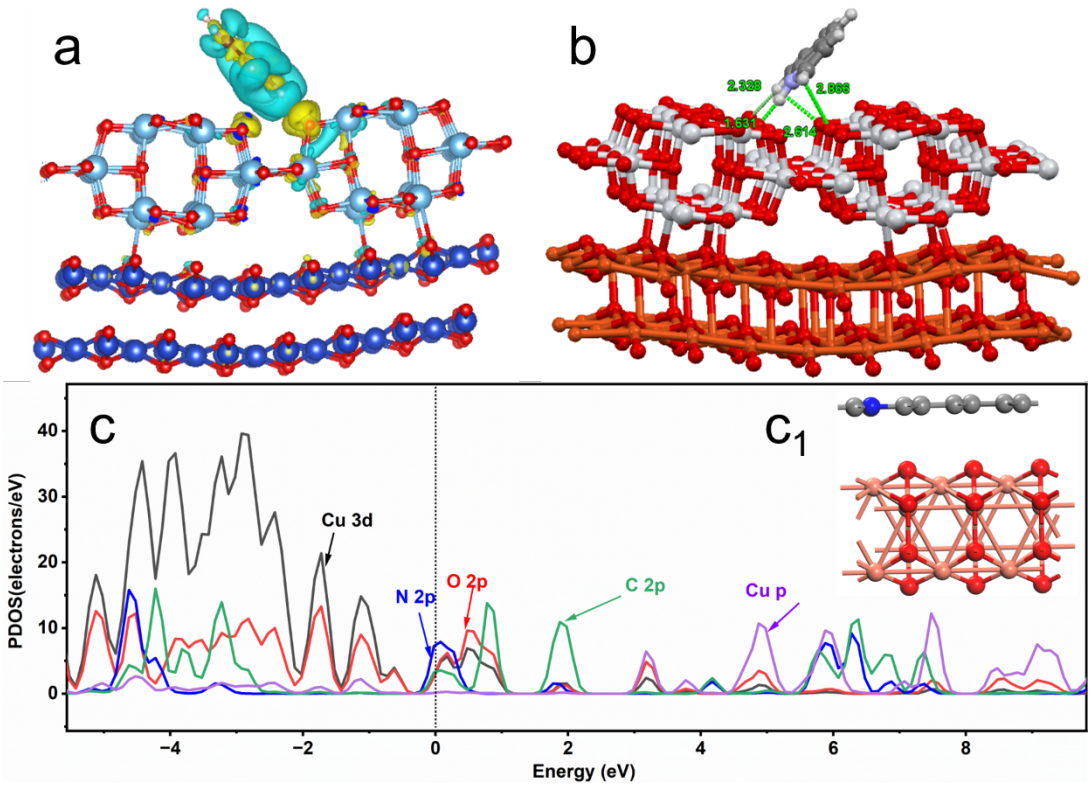

3. References

1 P. Giannozzi, O. Andreussi, T. Brumme, O. Bunau, M. Buongiorno Nardelli, M. Calandra, R. Car, C. Cavazzoni, D. Ceresoli, M. Cococcioni, N. Colonna, I. Carnimeo, A. Dal Corso, S. de Gironcoli, P. Delugas, R. A. DiStasio, A. Ferretti, A. Floris, G. Fratesi, G. Fugallo, R. Gebauer, U. Gerstmann, F. Giustino, T. Gorni, J. Jia, M. Kawamura, H. Y. Ko, A. Kokalj, E. Küçükbenli, M. Lazzeri, M. Marsili, N. Marzari, F. Mauri, N. L. Nguyen, H. V. Nguyen, A. Otero-de-la-Roza, L. Paulatto, S. Poncé, D. Rocca, R. Sabatini, B. Santra, M. Schlipf, A. P. Seitsonen, A. Smogunov, I. Timrov, T. Thonhauser, P. Umari, N. Vast, X. Wu and S. Baroni, *J. Phys.: Condens. Matter*, 2017, **29**, 465901.

2 P. Giannozzi, S. Baroni, N. Bonini, M. Calandra, R. Car, C. Cavazzoni, D. Ceresoli, G. L. Chiarotti, M. Cococcioni, I. Dabo, A. Dal Corso, S. de Gironcoli, S. Fabris, G. Fratesi, R. Gebauer, U. Gerstmann, C.

Gougoussis, A. Kokalj, M. Lazzeri, L. Martin-Samos, N. Marzari, F. Mauri, R. Mazzarello, S. Paolini, A. Pasquarello, L. Paulatto, C. Sbraccia, S. Scandolo, G. Sclauzero, A. P. Seitsonen, A. Smogunov, P. Umari and R. M. Wentzcovitch, *J. Phys.: Condens. Matter*, 2009, **21**, 395502.

3 J. P. Perdew, K. Burke and M. Ernzerhof, *Phys. Rev. Lett.*, 1996, **77**, 3865-3868.